Effect of oxidation on the gel properties of porcine myofibrillar proteins and their binding abilities with selected flavour compounds

Effect of oxidation on the gel properties of porcine myofibrillar proteins and their binding abilities with selected flavour compounds

Hui Shen[1], J. Stephen Elmore[2], Mouming Zhao[1,3], Weizheng Sun[1,2,3,*]

[1]*School of Food Science and Engineering, South China University of Technology, Guangzhou 510641, China*

[2]*Department of Food and Nutritional Sciences, University of Reading, Whiteknights, Reading RG6 6AP, UK*

[3]*Overseas Expertise Introduction Center for Discipline Innovation of Food Nutrition and Human Health (111 Center), Guangzhou 510641, China*

Corresponding author

Weizheng Sun, Professor

Tel/Fax: +86 20 22236089

E-mail: fewzhsun@scut.edu.cn

Abstract:

In this work, the effect of oxidation induced by hydroxyl radicals on the binding abilities of myofibrillar protein (MP) gels to aldehydes and ketones and their relationship with MP gel properties were investigated. Mild oxidation (0–0.2 mM H_2O_2) could induce partial unfolding of MP, thus slightly increasing the salt solubility of MP and enhancing the hardness of MP gels. MP suffering a higher oxidative attack could undergo a reduction in water-holding capacity, with increased mobility of water in MP gels. Oxidation could make MP gel more disordered. The ability of oxidised MP gels to bind to flavours decreased as the carbon chain length of the flavour compound increased. MP oxidation only significantly affected the binding of MP gels to hexanal, heptanal, and 2-octanone, while other flavour compounds were not affected.

Keywords: myofibrillar proteins; oxidation; gel properties; flavours release; water mobility

1. Introduction

The formation of protein gels in processed muscle foods is an important functionality that can affect the texture and sensory characteristics of the final meat products. Myofibrillar proteins (MP), as the major proteins in muscle, are excellent gelling agents that are largely responsible for the textural and structural characteristics of meat products (Xiong, Blanchard, Ooizumi, & Ma, 2010).

During meat storage or industrial processing, reactive oxygen species, which include superoxide anions, hydroxyl radicals, peroxyl radicals and lipid oxidation products, play a critical role in the accumulation of oxidative damage in proteins (Zhou, Zhao, Zhao, Sun, & Cui, 2014a). Types of oxidative damage to muscle proteins can include conformational changes, peptide chain scission and formation of amino acid derivatives or aggregates, leading to changes in physicochemical properties of proteins, which in turn alter the functional properties of proteins, such as gelation, emulsification and the capacity to bind flavours (Sun, Zhou, Sun, & Zhao, 2013; Xiong et al., 2010). The gel properties of MP, such as rheological properties, water-holding capacity (WHC), texture and microstructure change under oxidative stress (Xiong, Park, & Ooizumi, 2009).

Food acceptability by consumers is governed to a considerable extent by their organoleptic properties, and mostly by flavour perception (Gierczynski, Guichard, & Laboure, 2011). Volatile flavour release is largely determined by the tendency of volatile compounds to bind to other ingredients (particularly oils and protein) and by food microstructure (Guichard, 2002). As mentioned above, protein oxidation can affect meat products microstructure, especially gel quality. Some reports have evaluated the abilities of oxidised MP at different oxidation levels to bind to flavour compounds (Cao, Zhou, Wang, Sun, & Pan, 2018; Zhou et al., 2014a). Thus far,

investigations regarding the binding of oxidised MP gels to flavour compounds are limited. Modifying food microstructure can also control volatile release in foods (Mao, Roos, & Miao, 2014). Among flavours, the impacts of aldehydes and ketones are of particular interest because of their practical contribution in meat and meat products (Guichard, 2002). Therefore, it is necessary to investigate the behaviour of oxidised MP gels in binding to typical odour-active aldehydes and ketones, to establish the mechanism of flavour release in gelatinous meat products.

In this work, MP were exposed to a hydroxyl radical-generating system that is commonly involved in meat and meat products. Examination of the accompanying protein structural changes (sulfhydryl [SH] groups, surface hydrophobicity, salt solubility, particle size distribution) with the results of sodium dodecyl sulfate-polyacrylamide gel electrophoresis [SDS-PAGE]) and with gel properties (hardness, WHC, microstructure, low-field nuclear magnetic resonance [LF-NMR] relaxation time) was designed to investigate the influence of oxidative modification on MP and MP gels. The phenomena of oxidised MP gels binding to typical aldehyde and ketone compounds were evaluated using headspace analysis followed by gas chromatography–mass spectrometry. Moreover, selected aldehyde and ketone compounds of various chain lengths were used to evaluate the contributions of molecular structure to the binding phenomena. The relationship between MP gel properties and their binding abilities is discussed.

2. Materials and methods

2.1. Materials

Fresh porcine muscle (*longissimus dorsi*) was purchased from a local commercial abattoir (Guangzhou, China), where the pigs were slaughtered at approximately 6 months of age following standard industrial procedures. Fat and connective tissue were

removed before the separation of proteins. Pentanal, hexanal, heptanal, octanal, 2-pentanone, 2-heptanone, 5,5'-dithiobis-(2-nitrobenzoic acid) (DTNB) and piperazine-*N*,*N*-bis(2-ethanesulfonic acid) (PIPES) were purchased from Sigma-Aldrich Chemical Co. (St. Louis, MO); 2-hexanone, 2-octanone, propyl gallate and Trolox C were obtained from Aladdin (Shanghai, China). Bromophenol blue (BPB), thiourea, dithiothreitol and EDTA were obtained from Sinopharm Chemical Reagent Co., Ltd. (Shanghai, China). All other chemicals were of analytical reagent grade at minimum.

2.2. Preparation of MP

MP were extracted according to the method of Shen, Zhao and Sun (2019), with a slight modification. The pH of the MP suspension (0.1 M NaCl) in the last wash was adjusted to 6.25 before centrifugation (2000 *g*, 15 min, 4 °C). The concentrations of MP were measured by the Biuret method using bovine serum albumin as a standard. The MP pellet was kept on ice and used within 2 days.

2.3. Protein oxidation

MP were suspended (30 mg/mL) in a 15-mM PIPES buffer containing 0.6 M NaCl (pH 6.25). To oxidise them, MP suspensions were incubated at 4 °C for 24 h, using a hydroxyl radical-generating system. The hydroxyl radicals were produced by a 10-μM $FeCl_3$/100-μM ascorbic acid solution with 1 mM H_2O_2. Oxidation was terminated by adding propyl gallate/Trolox C/EDTA (1 mM each) (Xiong et al., 2009). The fresh MP suspension (30 mg/mL) without any hydroxyl radical-generating system or terminating agent was used as the control. The concentrations of MP in the following measurements were adjusted using a 15 mM PIPES buffer (pH 6.25) containing 0.6 M NaCl.

2.4. Total and reactive SH groups

Total SH contents were determined with a DTNB method with some modifications (Zhou, Zhao, Su, & Sun, 2014b). For determining the level of total SH groups, 1 mL

MP suspension (4 mg/mL) was mixed with 5 mL of 0.086 M Tris-Gly buffer (5 mM EDTA, 8 M urea, 0.6 M NaCl, pH 8.0) and 30 μL of 4 mg/mL DTNB (0.086 M Tris-Gly buffer, 5 mM EDTA, 0.6 NaCl, pH 8.0). After incubation at room temperature (25 ± 1 °C) for 30 min, the absorbance at 412 nm was recorded for the calculation of total SH groups using a molar extinction coefficient of 13,600 M^{-1} cm^{-1}. Reactive SH groups were prepared by incubating the reaction mixture in the absence of urea. The blank was run with 15-mM PIPES buffer (pH 6.25) containing 0.6-M NaCl.

2.5. Surface hydrophobicity

The surface hydrophobicity of the MP was measured by the hydrophobic chromophore BPB method (Chelh, Gatellier, & Santé-Lhoutellier, 2006) with a slight modification. This method can determine the surface hydrophobicity of MP, avoiding the solubilisation step of the myofibrils before the protein hydrophobicity determination. The MP suspension (1 mL, 4 mg/mL) was thoroughly mixed with 100 μL BPB (1 mg/mL) and kept at ambient temperature (25 ± 1 ℃) for 10 min before centrifugation (5000 *g*, 15 min, 25 °C). The absorbance of each supernatant (diluted for 10 times) was determined at 595 nm against a PIPES buffer blank. A sample with the same treatments in the absence of MP was used as the control. The index of surface hydrophobicity was expressed as the amount of bound BPB, and it was calculated using the following formula (1):

$$\text{BPB bound (μg)} = 100 \times (A_{control} - A_{sample})/A_{control} \quad (1)$$

2.6. Salt solubility and MP turbidity

Salt solubility of MP (10 mg/mL) and turbidity of MP suspensions (1 mg/mL) were determined according to Shen et al. (2019). The salt solubility of MPs was measured after centrifuging (5000 *g*, 25 °C) for 20 min to separate the salt-soluble fractions from

the insoluble fractions. The result was expressed as the percentage of initial protein concentration.

2.7. Particle size distributions

Particle size distributions of control and oxidised MP were measured with an integrated-laser light scattering instrument (Mastersizer 2000; Malvern Instruments Co. Ltd., Worcestershire, UK). The relative refractive index and absorption were set as 1.414 and 0.001, respectively. $D_{4,3}$ is the mean diameter in volume, and $D_{3,2}$ is the mean diameter in surface, called the 'Sauter diameter'. $D_{v,0.5}$ is the size for which 50% of the sample particles have a lower size and 50% have an upper size. The specific surface areas (square metres per gram) were also recorded.

2.8. Sodium dodecyl sulfate–polyacrylamide gel electrophoresis

Sodium dodecyl sulfate-polyacrylamide gel electrophoresis (SDS-PAGE) was performed on MP according to the method described by Zhou et al. (2014b) with a slight modification. Briefly, the MP suspension (4 mg/mL) was mixed in a 1:1 ratio with 50 mM Tris buffer (8 M urea, 2 M thiourea, 3% (w/v) SDS, 0.05% BPB and 20% (v/v) glycerine, pH 6.8) with or without 75 mM dithiothreitol. The samples were boiled for 4 min before centrifugation (10,000 *g*, 10 min, 25 °C). Next, 9 μL of each MP mixture were injected into each gel, comprising a 12% running gel and a 4% stacking gel. The electrophoresis was operated at a constant current of 25 mA using a Mini-PROTEAN 3 Cell apparatus (Bio-Rad Laboratories, Hercules, CA).

2.9. Gel properties

2.9.1. Preparation of heat-induced gels

For gelation, the control and oxidised MP (30 mg/mL) were prepared for gel property analyses according to the method of Zhou et al. (2014b). The MP suspensions were heated in a water bath from 25 °C to 72 °C at 1 °C/min increments (kept for 5 min at

53 °C and 10 min at 72 °C). After heating, the gels were immediately cooled to room temperature.

2.9.2. Gel hardness and WHC

Prior to the hardness measurements, gel samples were allowed to equilibrate at room temperature (25 ± 1°C) for 1 h. The hardness of MP gels was measured using a cylinder measuring probe (P/0.5S, 12.7 mm) attached to TA-XT Plus Texture Analyzer (Stable Micro Systems Ltd., Godalming, UK) at a constant probe speed of 1.0 mm/s at room temperature. The gel hardness was defined as the initial force required to rupture the gels.

WHC values for the gels were determined by a centrifugal method (Xia, Kong, Xiong, & Ren, 2010). Briefly, gel samples (3 g) were centrifuged at 4000 *g* for 15 min at room temperature. The WHC (%) was expressed using the final weight as a percentage of the weight before centrifugation (6000 *g*, 15 min, 4 °C).

2.9.3. Microstructure

The surface morphologies of control and oxidised MP gels were examined using field emission scanning electron microscopy (FE-SEM, model S-3400N; Hitachi, Japan) at an accelerator voltage of 15 kV. Cubic samples (approximately 3 × 3 × 3 mm) were prepared and snap-frozen in liquid N_2 (Zhou et al., 2014a). Before imaging, freeze-dried gel samples were mounted on a holder with double-sided adhesive tape and sputter-coated with gold (JFC-1200 fine coater; JEOL, Tokyo, Japan). Sample observation and photomicrography were performed at 500× and 2000× magnifications, respectively.

2.9.4. Low-field NMR relaxation time (T_2)

Low-field NMR relaxation measurements were performed according to a previous method (Zhang, Yang, Tang, Chen, & You, 2015) with some modifications.

Approximately 1.6 g of each gel sample formed in a 2 mL screw-cap chromatogram vial were placed inside a cylindrical glass tube (15 mm in diameter) and inserted into the NMR probe of a Niumag Benchtop Pulsed NMR analyser (Niumag PQ001; Niumag Electric Corporation, Shanghai, China). The analyser was operated at 32 ºC and a resonance frequency of 18 MHz. The T_2 was measured using the Carr-Purcell-Meiboom-Gill sequence with 4 scans, 8000 echoes, 2.0 s between scans, and 400 μs between pulses of 90° and 180°. The T_2 relaxation curves were fitted to a multi-exponential curve with the MultiExp Inv Analysis software (Niumag Electric Corporation, Shanghai, China), which used the inverse Laplace transform algorithm.

2.10. SPME–GC/MS

A stock solution containing all selected flavours (aldehydes and ketones) was freshly prepared in methanol (HPLC grade) and sealed in brown gas-tight glass bottles to prevent volatilising. The stock solution was then pipetted to control and oxidised MP suspensions (30 mg/mL), to a final concentration of 1 mg/kg for each flavour. Each mixture (8 mL protein/control solution + 50 μL stock solution) was placed in a 20-mL headspace vial and sealed with a polytetrafluoroethylene (PTFE)-faced silicone septum (Supelco, Bellefonte, PA, USA). For gelation, the control and oxidised MP gels were developed according to *Section 2.9.1*. The gel vials were stored at 25 °C for 16 h to allow equilibration.

The quantities of flavour compounds present in the headspace of gel vials were determined using solid-phase microextraction (SPME) followed by gas chromatography/mass spectroscopy (GC/MS) analysis according to the procedure described by Zhou et al. (2014a). The SPME parameters were as follows: 75 μm Carboxen/polydimethylsiloxane (CAR/PDMS) fibre (Supelco, Bellefonte, PA), equilibrated at 45°C for 20 min, extracted at 45°C for 30 min, desorbed at 220°C for 5

min. GC-MS conditions: TR-Wax column (30 m × 0.32 mm× 0.25 μm; J&W Scientific, Folsom, CA, USA) was used for separation. The carrier gas was high purity helium at a linear flow rate of 20.4 cm s^{-1}. The initial GC oven temperature was 38°C, held for 6 min, rising to 105°C at a rate of 6°C min^{-1}, then raised to 220°C at a rate of 15°C min^{-1}, and held at 220°C for 5 min. The mass spectrometry conditions were electron ionisation (EI) at 70 eV, electron multiplier voltage 350 V, scanning speed 3.00 scans/s, mass range *m/z* 33–350. The results were expressed as the difference in peak areas of flavour compounds between the oxidised MP gels and the control gel, calculated by the following equation (2):

Free flavour compound (%) = (peak area protein/peak area control) × 100 (2)

2.11. Statistical analysis

Data were expressed as means ± standard deviations of triplicate determinations. Statistical calculation was investigated by analysis of variance using SPSS 17.0 (SPSS, Inc., Chicago, IL). The means were compared using Duncan's multiple range test ($p < 0.05$).

3. Results and discussion

3.1. Total and reactive SH groups, surface hydrophobicity, salt solubility and turbidity

The loss of SH groups is one of the primary common characteristics of protein changes under oxidative attack (Xiong et al., 2009). As presented in **Table 1**, compared with the control, the total and reactive SH contents both decreased continuously upon oxidation with the increase of H_2O_2 concentrations ($p < 0.05$). MP are rich in SH groups that can be readily converted to disulphide linkages (S–S) upon oxidative stress (Cao, True, Chen, & Xiong, 2016). The decrease in total and reactive SH contents signified that the SH groups of cysteine were oxidised with the formation of S–S (Sante-

229 Lhoutellier, Aubry, & Gatellier, 2007). Cao et al. (2018) also suggested that SH groups
230 in G-actin were susceptible to hydroxyl radicals and easily changed into intermolecular
231 S–S. Hence, the generated hydroxyl radicals (0.05–5.0 mM H_2O_2) were responsible for
232 the decrease in total and reactive SH contents. In addition, contents of total and reactive
233 SH also significantly decreased ($p < 0.05$) in 0 mM H_2O_2 compared with the control,
234 which may be associated with oxidation induced by Fe^{3+} (Fe^{3+} catalyses H_2O_2 to
235 produce hydroxyl radicals).

236 For monitoring the subtle changes in physical and chemical states of proteins, surface
237 hydrophobicity is a suitable parameter (Sante-Lhoutellier et al., 2007). As shown in
238 **Table 1**, compared with the control, the hydrophobicity of MP (0 mM H_2O_2)
239 significantly increased ($p < 0.05$), implying that the addition of ascorbic acid, Fe^{3+} and
240 oxidative terminators may markedly increase the protein surface hydrophobicity. In
241 addition, surface hydrophobicity of MP gradually increased with the increase of H_2O_2
242 concentrations (0.05–5.0 mM), and the results were similar to those of some previous
243 reports (Cao et al., 2018; Sun et al., 2013). Chelh et al. (2006) suggested that the
244 increase of surface hydrophobicity could be attributed to the unfolding of MP, thus
245 exposing previously buried nonpolar amino acids at their surface. Oxidative damage
246 could induce partial unfolding of MP, thereby exposing the hydrophobic amino acids
247 that were normally buried in protein molecules (Estévez, 2011; Sante-Lhoutellier et al.,
248 2007). Moreover, the cleavage of certain peptides under oxidative stress may also result
249 in the enhancement of surface hydrophobicity (Pacifici, 1987).

250 Salt solubility can reflect the extent of proteins aggregation (Shen et al., 2019). As
251 shown in **Table 1**, compared with the control, salt solubility of MP revealed a slight
252 increase (1.19–3.43%; $p < 0.05$) with low concentrations of oxidant (0–0.2 mM), and
253 then exhibited a rapid decrease (0.59–51.36%; $p < 0.05$) for the further oxidant

treatments (0.5–5.0 mM). A slight oxidation could cause a subtle unfolding of proteins (Estévez, 2011), which may lead to better solubility in the salt solution. Nevertheless, with further increase in oxidant, the solubility of MP drastically decreased due to the stronger oxidative attack. This could be explained by the enhancement of surface hydrophobicity and the excessive protein aggregates (Sun, Li, Zhou, Zhao, & Zhao, 2014). The exposure of hydrophobic patches or individual groups, aggregation and polymerisation through S–S are all associated with the solubility decrease (Li, Xiong, & Chen, 2012).

Turbidity is attributed to the presence of protein aggregates. The turbidity of MP suspensions (**Table 1**) increased ($p < 0.05$) with the increased addition of H_2O_2 (0–5.0 mM), which accorded with the loss of SH and the increase of surface hydrophobicity. This indicated that the oxidised incubation could obviously enhance the aggregation behaviour of proteins. Under further analysis, this phenomenon was noted to be caused by the increased surface hydrophobicity due to the exposure of interior hydrophobic amino acid residues and the formation of intra- and intermolecular cross-links under oxidative attack (Li et al., 2012), thus leading to the turbidity increase of MP suspensions.

3.2. Particle size distributions

Particle size distributions can be used to monitor the aggregation behaviours of proteins under oxidative attack. As shown in **Fig. S1**, compared with the control, the particle size distribution of MP exhibited an obvious shift towards larger particles with the increase of H_2O_2 concentrations. Protein oxidation could promote intermolecular aggregation behaviours between protein molecules, thus increasing the particle size values (Xiong et al., 2009). Specifically, the $D_{3,2}$ value of MP after oxidation showed no significant difference ($p > 0.05$), while the values for other particle sizes ($D_{4,3}$ and

279 $D_{v,0.5}$) (**Table 2**) increased significantly ($p < 0.05$). The large droplets or droplet
280 aggregates have higher weight in the calculation of the $D_{4,3}$ value than they do in the
281 calculation of the $D_{3,2}$ value, and samples with similar $D_{3,2}$, but different $D_{4,3}$ would
282 result primarily from the amount of large droplets or droplet aggregates (Sun et al.
283 2014). This indicates that protein aggregation occurred after oxidation. Moreover, the
284 SH, surface hydrophobicity and turbidity analysis (**Table 1**) conformed to the
285 enhancement of association behaviours between protein molecules with the increase of
286 H_2O_2 concentrations, thereby enlarging the diameter of particles.

287 *3.3. SDS-PAGE*

288 The aggregation behaviours of the control and oxidised MP were further studied
289 using SDS-PAGE analysis (**Fig. S2**). In the absence of dithiothreitol, a large polymer
290 appeared at the top of the stack gel (**Fig. S2A**), suggesting the aggregation of MP. In
291 addition, MP aggregates induced by oxidative attack could form much larger aggregates
292 that could not enter the gel. Moreover, the intensities of the aggregation bands and the
293 aggregates all decreased and were not recovered in the presence of dithiothreitol (**Fig.**
294 **S2B**). This phenomenon indicated that the cross-links of the MP induced by oxidation
295 were not only through S–S but also through other covalent bonds (Cao et al., 2016). As
296 shown in the comparison between **Fig. S2A** and **Fig. S2B**, myosin heavy chain (MHC),
297 α-actinin and actin participated in the formation of aggregates.

298 *3.4. Gel properties*

299 *3.4.1. Hardness and WHC*

300 As aforementioned, oxidation had a pronounced effect on the physicochemical states
301 of MP. The hardness (**Fig. 1A**) and WHC (**Fig. 1B**) of the control and oxidised MP gels
302 were further evaluated. The mean hardness of the control gel was 21.9 ± 1.4 g and this
303 value was similar to that found by Xu, Han, Fei, and Zhou (2011). Compared with the

304 control, the hardness of mildly oxidised MP gels (0–0.2 mM H_2O_2) increased
305 significantly ($p < 0.05$). Due to the slightly unfolding of MP (salt solubility analysis), a
306 firmer matrix structure of MP gels may be formed during the heating process. Xiong et
307 al. (2010) also suggested that mild oxidation could promote protein network formation
308 and enhance the gelation of MP. Nevertheless, with more addition of H_2O_2 (0.5–5.0
309 mM), a significant decrease ($p < 0.05$) in gel hardness was observed, implying a weak
310 gel structure. In particular, heat-induced S–S bonds were regarded as an important
311 supporting force for the matrix structure of protein gels (Xiong et al., 2010). Hence, the
312 decrease of hardness may be attributed to the reduction of SH contents in MP (**Table**
313 **1**), thus leading to disordered aggregation replacing the ordered cross-links during
314 heating. Moreover, the decrease of salt solubility of MP could limit the ordered cross-
315 links within protein molecules during gelation.

316 Furthermore, WHC gave a quantitative indication of the amount of water maintained
317 within the protein gel structure, and this could reflect aspects of the spatial structure of
318 the gel (Zhou et al., 2014b). As shown in **Fig. 1B**, the control gel had the strongest
319 ability to retain water, and the WHC abilities of oxidised MP gels were gradually
320 weakened ($p < 0.05$) with an increase of H_2O_2 concentration (0–5.0 mM). As reported,
321 the structural integrity of myosin is of paramount importance for gelation and water
322 holding in meat (Deng et al., 2010). Oxidative damage to myosin could result in an
323 inferior gel network formation, causing lower elasticity with poor WHC in the gel
324 matrix. This was in good agreement with the surface hydrophobicity of MP (**Table 1**),
325 which could also reflect the affinity of proteins with water.

326 *3.4.2. Microstructure*

327 The changes in MP gel properties induced by oxidation were further investigated by
328 the measurements of surface morphologies, and the results are presented in **Fig. 2**. The

control gel appeared as a flat surface with several visible pores (**Fig. 2A** and **2B**), which indicated an ordered network structure due to protein stretching. At 2000 times magnification, the protein (control gel) exhibits a good cross-linked structure. Compared to the control, the mildly oxidised MP gels (0–0.2 mM H_2O_2) exhibited some fragments on the gel surface and a lower number of visible pores (**Fig. 2B**). The pore size of these gel was significantly reduced (× 500), and the original cross-linked structure was transformed into an aggregated particle structure, and the roughness is increased (× 2000), thereby yielding a firm pattern (hardness analysis). This phenomenon was attributed to the slight shrinkage of MP upon oxidation (Astruc, Gatellier, Labas, Lhoutellier, & Marinova, 2010). As a continuous increase of H_2O_2 (0.5–1.0 mM), aggregated particles and roughness further increased with the much more smaller pore size. Under 5 mM H_2O_2, the pores disappeared, and the fragments aggregated into clump structures. The surface morphologies of these gels revealed an uneven dense structure with aggregates and increased the roughness of the overlapped surface. This trend was in accordance with a previous observation (Zhou et al., 2014a). Formation of the surface structures of oxidised MP gels described previously could be attributed to the intra- and intermolecular cross-links and aggregates within proteins induced by oxiditive modification (Sun et al., 2014), thus leading to a disordered gel network structure during the heating process. In addition, the clump structures clearly aggregated into larger globular clusters when subjected to higher oxidative attack (2.5–5.0 mM H_2O_2), indicating an accelerated state of aggregation (**Fig. 2B**). These structural features implied that proteins under higher oxidative stress could undergo more steric modifications and contribute to the layered surface with bunched aggregation (Zhou et al., 2014a). These micrographs demonstrated the significant influences of oxidative treatments on protein gels. Moreover, these observations were in agreement with the

results of SH contents, surface hydrophobicity, turbidity and particle size distributions (**Table 1** and **Fig. S1**).

3.4.3. Relaxation time analysis

A fitted T_2 distribution was used to assess the relaxation time of hydrogen protons. The T_2 relaxation time distributions for the control and oxidised MP gels are shown in **Fig. 3**. Three peaks were noted for the control and in the gels with lower H_2O_2 concentrations (0–1.0 mM), while four peaks were noted for the gels with 2.5–5.0 mM H_2O_2. This meant that the protein gels under different oxidation levels could restrict water mobility at different magnitudes (Wang, Zhang, Bhandari, & Gao, 2016). The components with shorter relaxation time, T_{2b} and T_{21} (0–10 ms), represented the protons in macromolecular structures and those combined closely with the macromolecular structures, respectively. The component T_{22} (10–100 ms) was assigned to myofibrillar water and water within the protein structure. The last peak represented the extra-myofibrillar water (T_{23}) population, and this peak appeared between 300 and 2000 ms. Generally, the existence of four groups of water in MP gels was in agreement with some previous reports (Wang et al., 2016; Zheng et al., 2015).

With oxidation treatments, the relaxation time of T_{22} increased from 14.17 ms (control gel) to 16.30–28.48 ms (oxidised gels) with increasing H_2O_2 concentrations, and T_{23} increased from 613.59 ms (control and oxidised gels with 0–1.0 mM H_2O_2) to 705.48 ms (oxidised gels with 2.5–5.0 mM H_2O_2) (**Table 1S**). If the relaxation time is shorter, a smaller amount of mobile water is available, whereas the longer relaxation time implies a more mobile water fraction (Shao et al., 2016). Hence, the increased T_2 relaxation times suggested that oxiditive modifications could lead to a certain level of the immobilised water shifting to free water. This may be associated with the enhancement in hydrophobic trend arising from the increased surface hydrophobicity

379 of MP (**Table 1**). Also, the increased aggregation behaviours (**Fig. S1** and **Table 2**)
380 within MP molecules could decrease the surface areas in gels, thus resulting in a
381 decrease of macromolecule sites for WHC (Wang et al., 2016). Moreover, the relaxation
382 component T_{2b} had divided into another part (T_{21}) at higher H_2O_2 concentrations (2.5–
383 5.0 mM). This may be due to the degradation of MP upon higher oxidative stress, thus
384 contributing to greater mobility of the water in macromolecular structures. In addition,
385 McDonnell et al. (2013) suggested that certain side-chains, such as carboxyl-, amino-,
386 hydroxyl-, sulfhydryl-groups, and even carbonyl- and imido-groups, in proteins were
387 responsible for water binding. Therefore, the changes in T_{2b} relaxation time
388 corresponded to the availability of protein side-chains, as related to the oxidative
389 modifications. These phenomena accorded with the WHC results (**Fig. 1B**).

390 *3.5. Binding of MP gels to flavours*

391 A homologous series of aldehydes and ketones that varied in chain length was
392 selected to investigate the binding performances of MP gels under different oxidation
393 levels. In protein solution systems, the longer the carbon chain, the stronger the ability
394 of the flavour compound to bind to the protein. (Lou, Yang, Sun, Pan, & Cao, 2017;
395 Zhou et al., 2014a). By contrast, in this study, the free percentages of aldehydes and
396 ketones in each vial increased with the increase in carbon chain length (**Fig. 4**),
397 suggesting it was more difficult for the flavour compounds with longer chain length to
398 bind with MP gels, which can be related to the steric effect of the gel network structure.
399 In addition, consistent with the finding reported by Wang and Arntfield (2015), the free
400 percentage of all aldehydes was lower than that of the ketones with the same carbon
401 numbers in all vials (**Fig. 4**), suggesting that the binding abilities of oxidised MP gels
402 to aldehydes were stronger than to ketones. This was because of the higher molecular

activities and lower steric hindrance effects of carbonyl groups in aldehydes (Kühn et al., 2008).

As shown in Fig. 4A, the free percentages of hexanal and heptanal first decreased and then increased significantly ($p < 0.05$) with increased oxidation levels (0–5.0 mM). Although the free percentages of pentanal and octanal showed no significant changes ($p > 0.05$) at different oxidation levels, their trends were similar to those of hexanal and heptanal. The free percentages of ketones (Fig. 4B) (except for 2-octanone) showed no significant changes at different oxidation levels (0–5.0 mM). Volatile release from food is primarily controlled by the following two factors: the nature of aroma compounds (such as volatility and polarity) and the resistance to mass transfer from a food matrix to the air phase (Mao, Roots, & Miao, 2015). Protein oxidation increased the surface hydrophobicity and interaction of proteins (**Table 1**); the oxidised MP gels could exhibit higher binding phenomena through stronger interaction force (such as hydrophobic interaction) to flavours, thus reducing their free percentages in the headspace. However, the binding of a certain protein gel to flavours may also be influenced by the steric hindrance effect or mass transfer from MP gel. Therefore, flavours with a longer carbon chain could produce a stronger steric hindrance effect due to the gel network, thus preventing their access to the interior hydrophobic binding sites and thus increasing their presence in the headspace (Wang & Arntfield, 2015). As shown in **Fig. 2**, as the degree of oxidation increased, the homogeneous cross-linked MP gel network gradually changes to a granular shape, and gradually loses the gel network structure (the pore size of the gel network also gradually decreases), which increases the steric resistance of the MP gel, increasing the content of aroma components in the headspace vial. Therefore, the release of flavour compounds

depended on the balance between protein–flavour compound interactions and gel network–flavour compound limitations (Mao et al., 2014).

4. Conclusions

The influence of oxidative modifications induced by H_2O_2 (0–5.0 mM) on the properties of MP and MP gels was investigated. With an increase in H_2O_2 concentrations, MP tended to expose their interior hydrophobic amino acids and to lose SH content, thus leading to enhanced aggregation behaviours, an increase in surface hydrophobicity and turbidity and a larger particle size distribution. The covalent bonds in the MP aggregates included S–S, among others. Under oxidative attack, MP gels demonstrated decreased WHC and more mobility of water. Mild oxidation (0–0.5 mM H_2O_2) slightly increased the salt solubility of MP and the hardness of MP gels. The abilities of MP gels to bind to aldehydes and ketones decreased with the growth of the carbon chain. The release of flavours in a gel was different from that in a protein solution due to mass transfer from a gel matrix to the air phase and heat treatment. Under the balance between protein–flavour compound interaction and gel network–flavour compound steric hindrance, MP oxidation only significantly affected ($p < 0.05$) the binding between MP gels and hexanal, heptanal, and 2-octanone, while other flavour compounds were not affected significantly ($p > 0.05$).

Acknowledgement

This work was supported by the National Natural Science Foundation of China (31671870); the National Key R&D Program of China (2016YFD0401504); the China Scholarship Council (201906155018); the Science and Technology Program of Guangzhou (201807010102); the Science and Technology Program of Guangdong (2016B020203001) and the 111 Project (B17018).

452

453 **References**

454 Astruc, T., Gatellier, P., Labas, R., Lhoutellier, V. S., & Marinova, P. (2010).
455 Microstructural changes in *m. rectus abdominis* bovine muscle after heating. *Meat*
456 *Science*, *85*(4), 743–751.

457 Boland, A. B., Delahunty, C. M., & van Ruth, S. M. (2006). Influence of the texture of
458 gelatin gels and pectin gels on strawberry flavour release and perception. *Food*
459 *Chemistry*, *96*(3), 452–460.

460 Cao, Y., True, A. D., Chen, J., & Xiong, Y. L. (2016). Dual Role (Anti- and Pro-oxidant)
461 of Gallic Acid in Mediating Myofibrillar Protein Gelation and Gel *in Vitro*
462 Digestion. *Journal of Agricultural and Food Chemistry*, *64*(15), 3054–3061.

463 Chelh, I., Gatellier, P., & Santé-Lhoutellier, V. (2006). Technical note: A simplified
464 procedure for myofibril hydrophobicity determination. *Meat Science*, *74*(4), 681–
465 683.

466 Deng, Y., Rosenvold, K., Karlsson, A. H., Horn, P., Hedegaard, J., Steffensen, C. L.,
467 & Andersen, H. J. (2010). Relationship Between Thermal Denaturation of Porcine
468 Muscle Proteins and Water-holding Capacity. *Journal of Food Science*, *67*(5),
469 1642–1647.

470 Estévez, M. (2011). Protein carbonyls in meat systems: A review. *Meat Science*, *89*(3),
471 259–279.

472 Gierczynski, I., Guichard, E., & Laboure, H. (2011). Aroma perception in dairy
473 products: the roles of texture, aroma release and consumer physiology. A
474 review. *Flavour and Fragrance Journal*, *26*(3), 141–152.

475 Guichard, E. (2002). Interactions between flavor compounds and food ingredients and
476 their influence on flavor perception. *Food Reviews International*, *18*(1), 49–70.

Guinard, J. X., & Marty, C. (1995). Time‐intensity measurement of flavor release from a model gel system: effect of gelling agent type and concentration. *Journal of Food Science, 60*(4), 727–730.

Hansson, A., Giannouli, P., & van Ruth, S. (2003). The influence of gel strength on aroma release from pectin gels in a model mouth and *in vivo*, monitored with proton-transfer-reaction mass spectrometry. *Journal of Agricultural and Food Chemistry, 51*(16), 4732–4740.

Juteau-Vigier, A., Atlan, S., Deleris, I., Guichard, E., Souchon, I., & Trelea, I. C. (2007). Ethyl hexanoate transfer modeling in carrageenan matrices for determination of diffusion and partition properties. *Journal of Agricultural and Food Chemistry, 55*(9), 3577–3584.

Kühn, J., Considine, T., & Singh, H. (2008). Binding of flavor compounds and whey protein isolate as affected by heat and high pressure treatments. *Journal of Agricultural and Food Chemistry, 56*(21), 10218–10224.

Lee, H. A., Choi, S. J., & Moon, T. W. (2006). Characteristics of sodium caseinate- and soy protein isolate-stabilized emulsion-gels formed by microbial transglutaminase. *Journal of Food Science, 71*(6), C352–C357.

Li, C., Xiong, Y. L., & Chen, J. (2012). Oxidation-induced unfolding facilitates Myosin cross-linking in myofibrillar protein by microbial transglutaminase. *Journal of Agricultural & Food Chemistry, 60*(32), 8020–8027.

Lou, X., Yang, Q., Sun, Y., Pan, D., & Cao, J. (2017). The effect of microwave on the interaction of flavour compounds with G-actin from grass carp (Catenopharyngodon idella). *Journal of the Science of Food and Agriculture, 97*(12), 3917–3922.

Mao, L., Roos, Y. H., & Miao, S. (2014). Study on the rheological properties and volatile release of cold-set emulsion-filled protein gels. *Journal of Agricultural and Food Chemistry, 62*(47), 11420–11428.

Mao, L., Roos, Y. H., & Miao, S. (2015). Effect of maltodextrins on the stability and release of volatile compounds of oil-in-water emulsions subjected to freeze–thaw treatment. *Food Hydrocolloids, 50,* 219–227.

McDonnell, C. K., Allen, P., Duggan, E., Arimi, J. M., Casey, E., Duane, G., & Lyng, J. G. (2013). The effect of salt and fibre direction on water dynamics, distribution and mobility in pork muscle: a low field NMR study. *Meat Science, 95*(1), 51–58.

O'Neill, T. E., & Kinsella, J. E. (1987). Binding of alkanone flavors to β-lactoglobulin: effects of conformational and chemical modification. *Journal of Agricultural and Food Chemistry, 35*(5), 770–774.

Pacifici, R. E. (1987). Protein damage and degradation by oxygen radicals. *Journal of Biological Chemistry, 262*(20), 9902–9907.

Sante-Lhoutellier, V., Aubry, L., & Gatellier, P. (2007). Effect of oxidation on *in vitro* digestibility of skeletal muscle myofibrillar proteins. *Journal of Agricultural & Food Chemistry, 55*(13), 5343–5348.

Shao, J. H., Deng, Y. M., Song, L., Batur, A., Jia, N., & Liu, D. Y. (2016). Investigation the effects of protein hydration states on the mobility water and fat in meat batters by LF-NMR technique. *LWT - Food Science and Technology, 66,* 1–6.

Shen, H., Zhao, M., & Sun, W. (2019). Effect of pH on the interaction of porcine myofibrillar proteins with pyrazine compounds. *Food Chemistry, 287,* 93–99.

Sun, W., Li, Q., Zhou, F., Zhao, H., & Zhao, M. (2014). Surface characterization of oxidized myofibrils using X-ray photoelectron spectroscopy and scanning electron microscopy. *Journal of Agricultural & Food Chemistry, 62*(30), 7507–7514.

526 Sun, W., Zhou, F., Sun, D.-W., & Zhao, M. (2013). Effect of Oxidation on the
527 Emulsifying Properties of Myofibrillar Proteins. *Food and Bioprocess Technology, 6*(7), 1703–1712.
528
529 Wang, K., & Arntfield, S. D. (2015). Binding of selected volatile flavour mixture to
530 salt-extracted canola and pea proteins and effect of heat treatment on flavour
531 binding. *Food Hydrocolloids, 43*, 410–417.
532 Wang, K., & Arntfield, S. D. (2016). Modification of interactions between selected
533 volatile flavour compounds and salt-extracted pea protein isolates using chemical
534 and enzymatic approaches. *Food Hydrocolloids, 61*, 567–577.
535 Wang, L., Zhang, M., Bhandari, B., & Gao, Z. (2016). Effects of malondialdehyde-
536 induced protein modification on water functionality and physicochemical state of
537 fish myofibrillar protein gel. *Food Research International, 86*, 131–139.
538 Xia, X., Kong, B., Xiong, Y., & Ren, Y. (2010). Decreased gelling and emulsifying
539 properties of myofibrillar protein from repeatedly frozen-thawed porcine
540 longissimus muscle are due to protein denaturation and susceptibility to
541 aggregation. *Meat Science, 85*(3), 481–486.
542 Xiong, Y., Blanchard, S. P., Ooizumi, T., & Ma, Y. (2010). Hydroxyl radical and ferryl-
543 generating systems promote gel network formation of myofibrillar protein.
544 *Journal of Food Science, 75*(2), C215–C221.
545 Xiong, Y. L., Park, D. K., & Ooizumi, T. (2009). Variation in the cross-linking pattern
546 of porcine myofibrillar protein exposed to three oxidative environments. *Journal
547 of Agricultural & Food Chemistry, 57*(1), 153–159.
548 Xu, X. L., Han, M. Y., Fei, Y., & Zhou, G. H. (2011). Raman spectroscopic study of
549 heat-induced gelation of pork myofibrillar proteins and its relationship with
550 textural characteristic. *Meat Science, 87*(3), 159–164.

551 Zhang, Z., Yang, Y., Tang, X., Chen, Y., & You, Y. (2015). Chemical forces and water
552 holding capacity study of heat-induced myofibrillar protein gel as affected by high
553 pressure. *Food Chemistry, 188*, 111–118.
554 Zheng, H., Xiong, G., Han, M., Deng, S., Xu, X., & Zhou, G. (2015). High
555 pressure/thermal combinations on texture and water holding capacity of chicken
556 batters. *Innovative Food Science & Emerging Technologies, 30*, 8–14.
557 Zhou, F., Zhao, M., Su, G., & Sun, W. (2014b). Binding of aroma compounds with
558 myofibrillar proteins modified by a hydroxyl-radical-induced oxidative system.
559 *Journal of Agricultural & Food Chemistry*, *62*(39), 9544–9552.
560 Zhou, F., Zhao, M., Zhao, H., Sun, W., & Cui, C. (2014a). Effects of oxidative
561 modification on gel properties of isolated porcine myofibrillar protein by peroxyl
562 radicals. *Meat Science, 96*(4), 1432–1439.

563 **Table 1** Total and reactive sulfhydryl groups, surface hydrophobicity, salt solubility and turbidity of the control and oxidised MP

H_2O_2 (mM)	Total sulfhydryl (nmol/mg protein)	Reactive sulfhydryl (nmol/mg protein)	Surface hydrophobicity (μg BPB)	Salt solubility (%)	Turbidity (FTU)
Control	9.02 ± 0.12g	8.45 ± 0.09h	22.75 ± 1.22a	83.57 ± 1.39d	83.11 ± 0.82a
0.0	8.30 ± 0.04f	6.35 ± 0.05g	38.02 ± 0.86bc	84.57 ± 0.46de	84.27 ± 0.58a
0.05	8.19 ± 0.02f	5.99 ± 0.07f	36.57 ± 2.15b	86.43 ± 1.09e	87.13 ± 0.56b
0.2	7.99 ± 0.05e	5.56 ± 0.11e	38.59 ± 0.85c	86.39 ± 0.66e	90.44 ± 2.37c
0.5	6.95 ± 0.03d	3.24 ± 0.11d	41.26 ± 0.72d	83.08 ± 0.94d	91.71 ± 1.99c
1.0	5.87 ± 0.03c	2.84 ± 0.07c	42.47 ± 0.34d	79.28 ± 2.73c	92.74 ± 0.91c
2.5	3.52 ± 0.11b	1.82 ± 0.05b	46.23 ± 0.71e	52.23 ± 0.96b	97.05 ± 1.47d
5.0	1.01 ± 0.05a	0.37 ± 0.03a	49.88 ± 1.08f	40.65 ± 1.02a	96.70 ± 0.90d

564 Values in the same column with different letters were significantly different ($p < 0.05$).

565 **Table 2** Average particle size ($D_{3,2}$ and $D_{4,3}$) and span of the control and oxidised MP

H_2O_2 (mM)	$D_{3,2}$ (μm)	$D_{4,3}$ (μm)	$D_{v,0.5}$ (μm)	Span
Control	41.55 ± 1.51a	99.58 ± 2.76a	69.57 ± 1.63a	2.89 ± 0.05ab
0.0	50.93 ± 0.84b	119.53 ± 1.09b	86.79 ± 1.30b	2.80 ± 0.09a
0.05	51.47 ± 1.80b	120.12 ± 3.39bc	86.18 ± 3.36b	2.84 ± 0.06a
0.2	51.06 ± 1.58b	121.22 ± 3.70bc	87.00 ± 3.40b	2.86 ± 0.03a
0.5	51.53 ± 1.19b	125.19 ± 2.46bc	87.57 ± 2.03b	3.01 ± 0.03bc
1.0	48.80 ± 1.90b	126.49 ± 4.66c	87.62 ± 3.70b	3.11 ± 0.03cd
2.5	50.72 ± 2.12b	138.31 ± 4.05d	96.93 ± 3.48c	3.12 ± 0.06cd
5.0	51.77 ± 2.21b	146.12 ± 5.07e	101.82 ± 4.95c	3.18 ± 0.17d

566 Values in the same column with different letters were significantly different ($p < 0.05$).

Figure Captions:

Fig. 1. Hardness (A) and WHC (B) of the control and oxidised MP gels. Different letters denote a significant difference between means ($p < 0.05$).

Fig. 2. Scanning electron microscope micrographs at ×500 (A) and ×2000 (B) magnification of the control and oxidised MP gels. Scale bars indicate 100 μm (A) and 20 μm (B).

Fig. 3. Distributions of T_2 relaxation times of the control and oxidised MP gels.

Fig. 4. Binding phenomena of the control and oxidised MP gels to selected aldehydes (A) and ketones (B). Results were expressed as percentage of free flavours found in the headspace of the control gel. Capital letters denote significant differences ($p < 0.05$) in flavour compound release for a same oxidant concentration, while lowercase letters denote significant differences ($p < 0.05$) in compound release between oxidant concentrations.

580

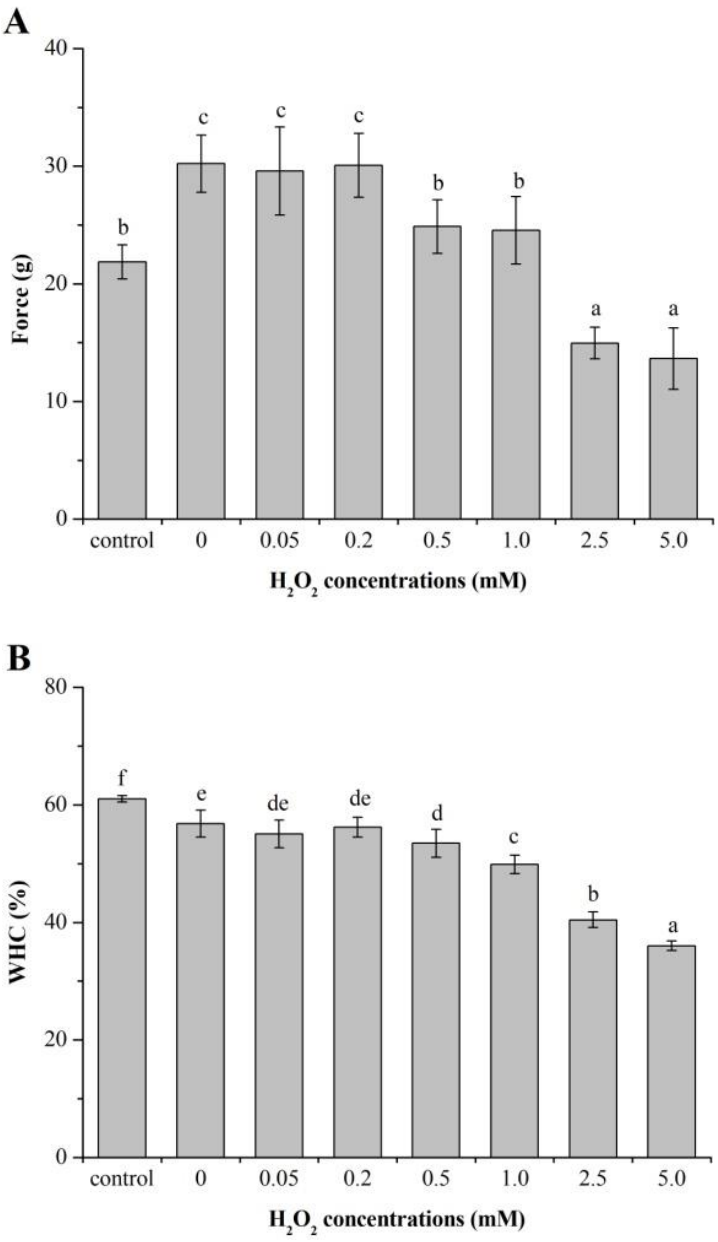

581

582 **Fig. 1**

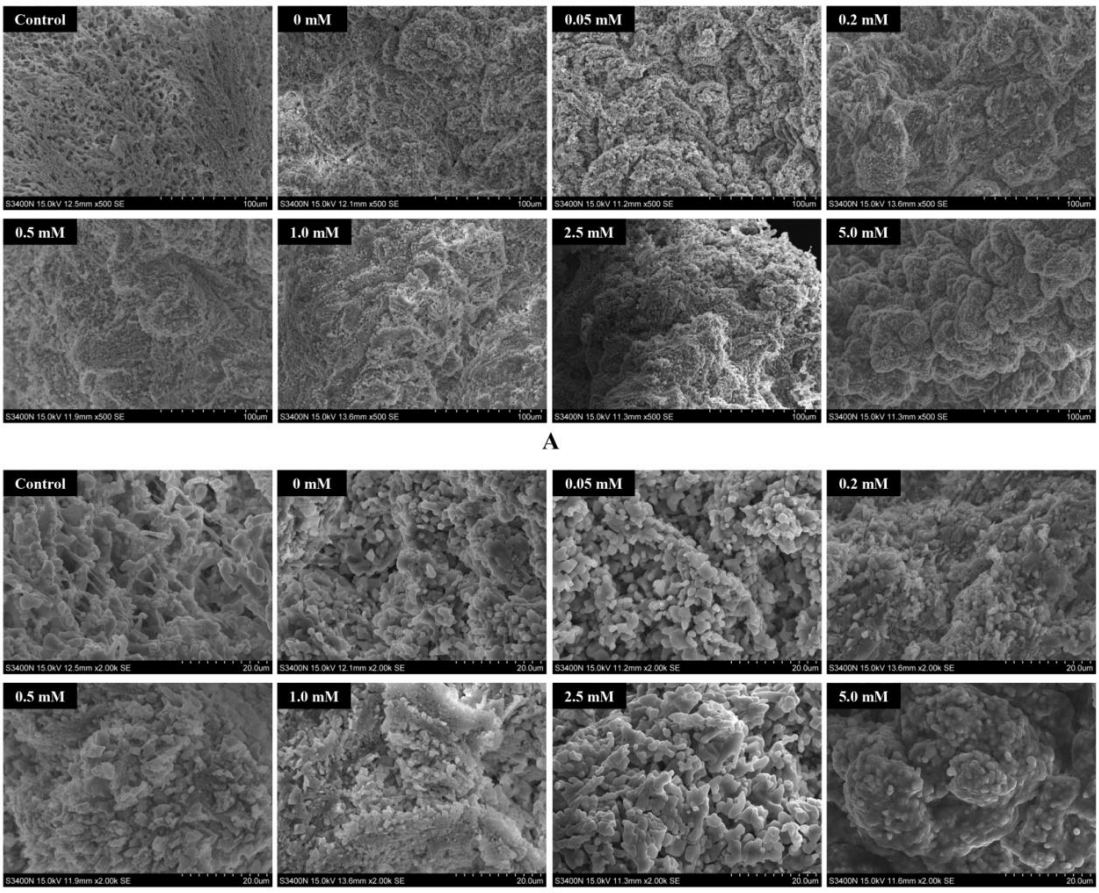
Control
0 mM
0.05 mM
0.2 mM
0.5 mM
1.0 mM
2.5 mM
5.0 mM
A
Control
0 mM
0.05 mM
0.2 mM
0.5 mM
1.0 mM
2.5 mM
5.0 mM
B

583

584 **Fig. 2**

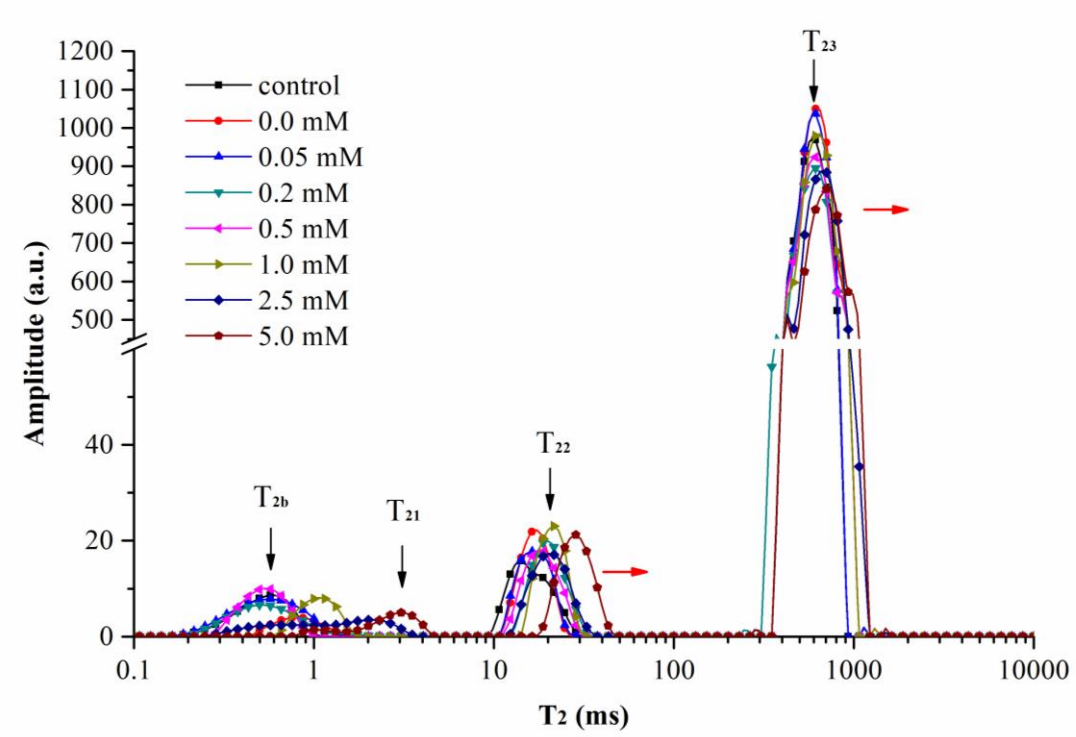
Amplitude (a.u.)
T2 (ms)
control
0.0 mM
0.05 mM
0.2 mM
0.5 mM
1.0 mM
2.5 mM
5.0 mM
T2b
T21
T22
T23

585

586 **Fig. 3**

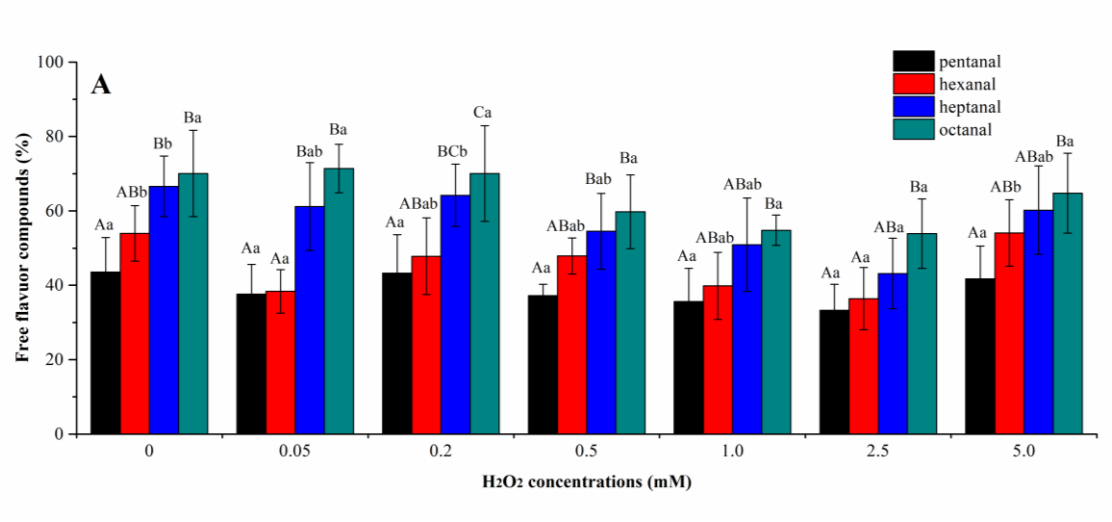

587

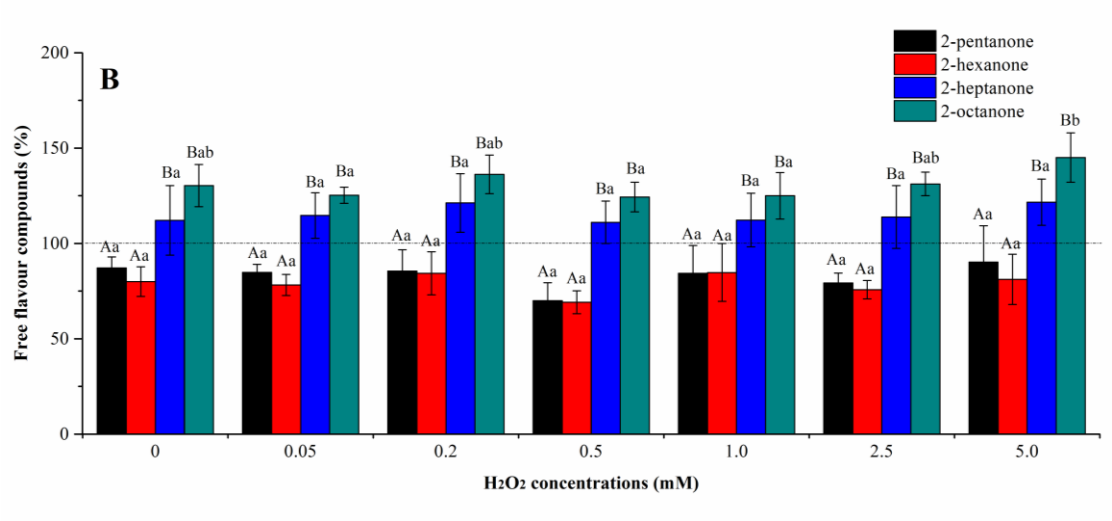

588

589 **Fig. 4**